PERGAMON

International Journal of Heat and Mass Transfer 44 (2001) 3273–3280

International Journal of HEAT and MASS TRANSFER

www.elsevier.com/locate/ijhmt

Conjugate natural convection in a square enclosure containing volumetric sources

A. Liaqat, A.C. Baytas *

Istanbul Technical University, Institute for Nuclear Energy, 80626 Maslak, Istanbul, Turkey

Received 18 February 2000; received in revised form 27 July 2000

Abstract

Laminar natural convection flow in a square enclosure having thick conducting walls has been analysed numerically. Enclosing walls are considered to have finite conductive properties. Problem has been analysed using control volume approach and employing ghost nodes at the solid fluid interface. Outsides of the walls are kept at constant temperature. Square cavity is assumed to be filled with a Bousinessq fluid with a Prandtl number of 7.0 containing uniform volumetric sources. Rayleigh number is varied from 10^7 to 10^{12}. For special cases, benchmark results compare very well with the results from open literature. Isotherms, streamlines and wall Nusselt numbers are obtained and scrutinised. Results show a significant change in the buoyant flow parameters as compared to conventional non-conjugate investigations. Especially, it has been shown that walls having high thermal diffusivity are much better suited, if the cooling of the enclosed fluid is intended.

Keywords: Conjugate; Convection; Enclosure flows

1. Introduction

Natural convection in enclosures has attracted considerable interest of investigators. Applications of such analysis range from building design, design of furnaces, design of nuclear reactors and others. Analysis of buoyant flow in internally heated enclosures is especially useful for nuclear and chemical industries.

Many experimental and numerical studies are available in open literature for buoyant flows in different types of cavities containing volumetric heat sources. Steinberner et al. [1] reported an experimental study of natural convection heat transfer with internal heat sources for a Ra number varying from 5×10^{10} to 3×10^{13}. Liaqat and Baytas [2] reported detailed analysis of high Rayleigh number natural convection flow in a square cavity and buoyant flow for Rayleigh numbers from 10^7 to 10^{12} was analysed. Kulacki et al. [3] investigated the natural convection in a horizontal fluid layer containing internal heat sources, the experimental observations were carried out for Ra number from 114.0 to 1.8×10^6. Emara et al. [4] performed a numerical analysis of a heat generating fluid layers for a Ra number range of 5.0×10^4 to 5.0×10^8. Tzanos et al. [5] performed a numerical simulation of natural convection in a cylindrical pool of heat generating fluid, the analysis was carried out for Ra numbers from 1.33×10^9 to 8.69×10^{11}. Bergholz [6] solved boundary layer equations analytically to study the natural convection in a heat generating fluid in a closed Cartesian cavity. Boundary layer analysis was used to obtain the equations valid near the walls and corresponding system of equations valid in the core of the cavity. May [7] presented a detailed numerical investigation of buoyant flow in a square enclosure having internal heating sources for a Ra number range of 10^4 to 1.5×10^5. Baytas [8] analysed the effect of periodic sources on the buoyancy driven flow and heat transfer characteristics. An experimental study to analyse the effect of inclination angle upon buoyant flow was reported by Lee et al. [9], system was analysed for a square cavity with uniform internal sources for Ra number from 1.0×10^4 to 1.5×10^5. Nourgaliev et al. [10] numerically analysed the

* Corresponding author. Tel.: +90-212-285-3945; fax: +90-212-285-3884.

E-mail address: baytas@itu.edu.tr (A.C. Baytas).

0017-9310/01/$ - see front matter
PII: S 0 0 1 7 - 9 3 1 0 (0 0) 0 0 3 4 5 - 8

Nomenclature

A	the ratio of thermal diffusivities, α_w/α_f
C_p	specific heat at constant pressure (kJ/kg K)
D	horizontal/vertical dimension of the cavity (m)
g	gravitational acceleration (m/s^2)
K	the ratio of thermal conductivities (k_w/k_f)
k_w	thermal conductivity of the wall (W/m K)
k_f	thermal conductivity of the fluid (W/m K)
Nu_a	average Nusselt number, Eq. (9)
Nu_l	local Nusselt number, Eq. (8)
n	direction normal to the wall
Pr	Prandtl number, $(=\nu/\alpha)$
q'''	uniform volumetric heat source (W/m^3)
Ra	Rayleigh number, $(=g\beta q''' D^5/k_f\alpha\nu)$
s_i	spatial position, Eq. (10)
t_i	physical time (s)
t	thickness of the wall (m)
T	dimensional temperature (K)
ΔT	reference temperature (K)
u, v	velocity components in x, y directions (m/s)
U, V	dimensionless velocity components in X, Y directions
x, y	Cartesian coordinates (m)
X, Y	dimensionless Cartesian coordinates

Greek symbols

α_w	thermal diffusivity of the wall (m^2/s)
α_f	thermal diffusivity of the fluid (m^2/s)
α_s	rate of grid stretching, Eq. (10)
β	coefficient of thermal expansion of the fluid (K^{-1})
θ	dimensionless temperature
υ	kinematic viscosity of the fluid (m^2/s)
ρ	density of the fluid (kg/m^3)
τ	dimensionless time

Subscripts

i, j	grid points indices
w	value on the wall

natural convection inside a rectangular cavity containing heat generating fluid.

In all above mentioned studies walls are considered to be isothermal and of zero thickness thus neglecting the conduction in the wall. But in practical cases all enclosures have somewhat thick walls with finite conductivities, leading to conjugate problem. Most of the conjugate heat transfer analysis that has been performed to date includes very simple geometries, such as flow between heated parallel plates and axisymmetric flow in a heated pipe. A review of some of these studies has been presented by WanLai et al. [11]. Kaminski et al. [12] numerically analysed the effect of conduction in one of the vertical walls on natural convection flow in a square enclosure. The results were compared with the results obtained from approximate methods and with empirical correlation, which were in good agreement. This study has been utilised for benchmarking in the present analysis, which shows a good agreement between both results.

Main aim of the present analysis is to investigate the nature of the buoyant flow in a square enclosure when all the four containing walls are thick and have finite conductive properties.

2. Mathematical formulation

Fig. 1 shows the details of the physical situation to be analysed. Cavity is square and all the walls are thick having constant outside temperature, i.e., rigid walls with finite conductivities and all velocities are zero at the walls (non-slip boundary condition). The internal heat source is distributed uniformly within the cavity. The flow is considered to be laminar two-dimensional (2D). The fluid is Newtonian and Bousinessq approximation is invoked for the fluid density, all other properties are assumed to be constant.

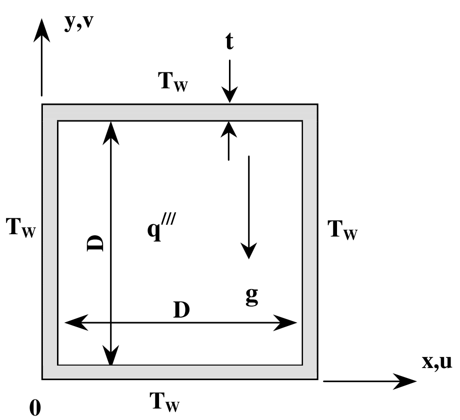

Fig. 1. Schematic diagram of the physical situation.

The governing dimensionless equations are unsteady Navier–Stokes and energy equations for laminar free convection as given below.

Equations for fluid region of the enclosure:

$$\frac{\partial U}{\partial \tau} + U\frac{\partial U}{\partial X} + V\frac{\partial U}{\partial Y} = -\frac{\partial P}{\partial X} + \frac{Pr}{(RaPr)^{2/5}}\nabla^2 U, \tag{1}$$

$$\frac{\partial V}{\partial \tau} + U\frac{\partial V}{\partial X} + V\frac{\partial V}{\partial Y} = -\frac{\partial P}{\partial Y} + \frac{Pr}{(RaPr)^{2/5}}\nabla^2 V + \theta, \tag{2}$$

$$\frac{\partial\theta}{\partial\tau} + U\frac{\partial\theta}{\partial X} + V\frac{\partial\theta}{\partial Y} = \frac{1}{(RaPr)^{2/5}}\nabla^2\theta + (RaPr)^{-1/5}. \tag{3}$$

Equation for solid region of the enclosure: The two-dimensional temperature distribution in the walls is governed by the heat conduction equation, which in the dimensionless form is given below

$$\frac{\partial\theta}{\partial\tau} = \frac{\alpha_w}{\alpha_f}\frac{1}{(RaPr)^{2/5}}\nabla^2\theta. \tag{4}$$

These equations has been non-dimensionalised by using non-dimensional variables as listed below:

$$(X,Y) = \frac{x,y}{D}, \quad (U,V) = \frac{u,v}{(\alpha_f/D)(RaPr)^{2/5}},$$
$$\theta = \frac{T - T_w}{\Delta T}, \quad \tau = \frac{t_i\alpha}{D^2}(RaPr)^{2/5}, \tag{5}$$
$$P = \frac{pD^2}{\rho_0\alpha_f^2(RaPr)^{4/5}}, \quad \Delta T = \frac{q'''D^2}{k_f(RaPr)^{1/5}}.$$

The corresponding initial and boundary conditions are:

$$\begin{aligned} &\text{for } \tau \leqslant 0 \text{ for whole space } \theta = U = V = 0,\\ &\text{for } \tau > \mathbf{0} : U = V = \mathbf{0} \text{ at all walls and in solid region},\\ &\text{for } \tau > \mathbf{0} : \theta = \mathbf{0} \text{ at } X = 0, 1.1 \text{ and } Y = 0, 1.1\\ &. \end{aligned} \tag{6}$$

At the interface the temperature and the heat flux must be continuous. The latter condition could be expressed as

$$\left(\frac{\partial\theta}{\partial n}\right)_{\text{fluid}} = \frac{k_w}{k_f}\left(\frac{\partial\theta}{\partial n}\right)_{\text{wall}}, \tag{7}$$

where n is in X or Y direction (normal to the interface).

Heat transfer local Nusselt numbers are defined by the following expression:

$$Nu_l = \left|\frac{\partial\theta}{\partial n}\right|_w. \tag{8}$$

The average Nusselt numbers are defined as follows:

$$Nu_a = \int_{0.05}^{1.05}\left|\frac{\partial\theta}{\partial n}\right|_w \mathrm{d}n, \tag{9}$$

where n denotes the X or Y direction.

2.1. Parameters of the problem

The complete conjugate problem is governed by five dimensionless variable parameters. These are the Rayleigh number Ra, the Prandtl number Pr, the dimensionless wall thickness t/D, the conductivity ratio K and thermal diffusivity ratio A. For the present analysis Pr number was taken fixed as 7.0 while Ra number was varied from 10^7 to 10^{12}. Dimensionless thickness ratio was kept constant as 0.05. For the present analysis three separate cases were studied depending upon the values of conductivity ratio and thermal diffusivity ratio. Table 1 summarises these cases and respective variable values. Case 2 was considered to represent the stainless steel (SS-304) wall material and water as inside fluid. Properties for these materials were taken to be constant at 20°C.

3. Solution procedure

Present analysis is based upon control volume method to discretise the governing non-dimensional equations as discussed by Patankar [13]. Staggered grid procedure was used in primitive variables with a Power Law differencing scheme for convection terms, for the fluid domain. To handle the pressure, temperature and velocity coupling of governing equations, SIMPLER algorithm was utilised. The method was applied to conjugate problem by employing ghost nodes at the fluid solid interface as described by WanLai et al. [11]. In this method the flow in the cavity and conduction in the walls are solved simultaneously. This is achieved by employing the ghost nodes at the solid fluid interface, as shown schematically in Fig. 2. The energy and momentum equations were solved by alternating direction implicit (ADI) method. ADI lead to triangular matrix which was easy to solve with tri-diagonal matrix algorithm (TDMA) as described by Versteeg [14]. Pressure correction equation used in SIMPLER algorithm was solved by point successive overrelaxation (PSOR) procedure. Optimum over-relaxation parameter for the pressure correction equation was found to be 1.93 for a non-uniform grid of 71×71. For each wall total 10 grids were used inside the solid region while for fluid region 51 grids were provided. High density of grids was provided near the solid fluid interface in order to resolve

Table 1
Summary of different cases analysed for the conjugate problem

	K	A	Max. Ra no. considered	Comments
Case 1	1.0	1.0	1.0×10^9	Fluid and solid are same
Case 2	21.0	24.0	1.0×10^{11}	Solid – stainless steel; fluid – water
Case 3	∞	–	1.0×10^{12}	Non-conjugate problem

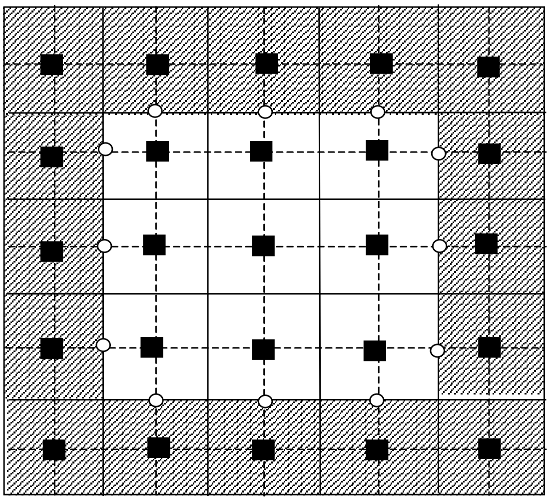

Fig. 2. Schematic diagram showing main and ghost nodes.

the boundary layer properly. The non-uniformity of the grid is described by the relation, Baytas [8]

$$S_{i+1} = S_i + \alpha_s^i \Delta, \tag{10}$$

where S_i represents the spatial location of the grid line, $\Delta(= 0.005)$ the step size and α_s the stretching parameter. The density of the grid is higher near the walls where sharp gradients of temperature and velocity are expected. Accuracy tests for mesh sensitivity analysis of two- dimensional square cavity (non-conjugate) were performed for flow domain in Liaqat and Baytas [2] for high Ra number range of 10^7–10^{12}. Optimisation of the results upon the time step was performed and a suitable time step was selected for each Ra number. The convergence of the pressure correction equation was declared when the following criterion was satisfied

$$\sum_{i,j} \left| P_{i,j}^{n+1} - p_{i,j}^{n} \right| \leqslant 10^{-6}.$$

The convergence of computations is established by utilising the following relation for the temperature distribution

$$\sum \left| T_{i,j}^{n+1} - T_{i,j}^{n} \right| \Big/ T_{\max} \leqslant 10^{-4},$$

where $T_{\max}$ is the maximum temperature in the cavity for each time step.

3.1. Benchmark solutions

Accuracy of the program developed by the authors was checked by preparing the benchmark solutions both for non-conjugate and conjugate problems. In case of non-conjugate analysis, well-known benchmark solution of Vahl Davis [15] was used for low Ra numbers. Results from Lage et al. [16] were utilised for benchmarking at high Ra number range. These benchmark results are shown in Table 2. For conjugate problem benchmark solution has been obtained by

Table 2
Comparison of the present numerical solution with some previous numerical average Nusselt numbers

Ra	Grid	Lage et al. [16]	Vahl Davis [15]	Present
10^4	41×41[a]		2.242	2.254
10^5	41×41[a]		4.564	4.616
10^6	41×41[a]	9.2	9.27	8.973
10^7	51×51[b]	17.9		17.051
10^8	51×51[b]	31.8		32.811
10^9	51×51[b]	62.7		68.381

[a] Uniform grid.
[b] Non-uniform grid ($\alpha_s = 1.117$).

Table 3
Benchmark solution for conjugate problem

Gr	K	Kaminski et al. [12] Nu_a	Present Nu_a
1×10^3	1.0	0.87	0.877
	∞	1.06	1.066
1×10^5	1.0	2.08	2.082
	∞	4.08	4.122
1×10^6	1.0	2.87	2.843
	∞	7.99	8.066

using results of Kaminski et al. [12]. Table 3 shows the excellent comparison between the results. Liaqat and Baytas [2] also prepared a benchmark solution for validation with the well-known experimental study of Steinberner [1].

4. Results and discussion

During present analysis of the conjugate problem different cases and respective maximum Ra number considered are summarised in Table 1.

4.1. Isotherms and streamlines

For $Ra = 10^7$ isotherms and streamlines obtained for the three cases are shown in Fig. 3. A low temperature dip near the upper left corner is visible in Fig. 3(a); this dip varies in position and magnitude with time creating oscillations in the flow and temperature fields. Fig. 3(b) indicates for the result of case 2. At $Ra = 10^7$, most developed flow pattern is obtained for case 3 as is shown in Fig. 3(c). Maximum dimensionless temperature inside the enclosure is obtained for case 1 (Fig. 3(a)), advocating poor heat transfer from the containing walls.

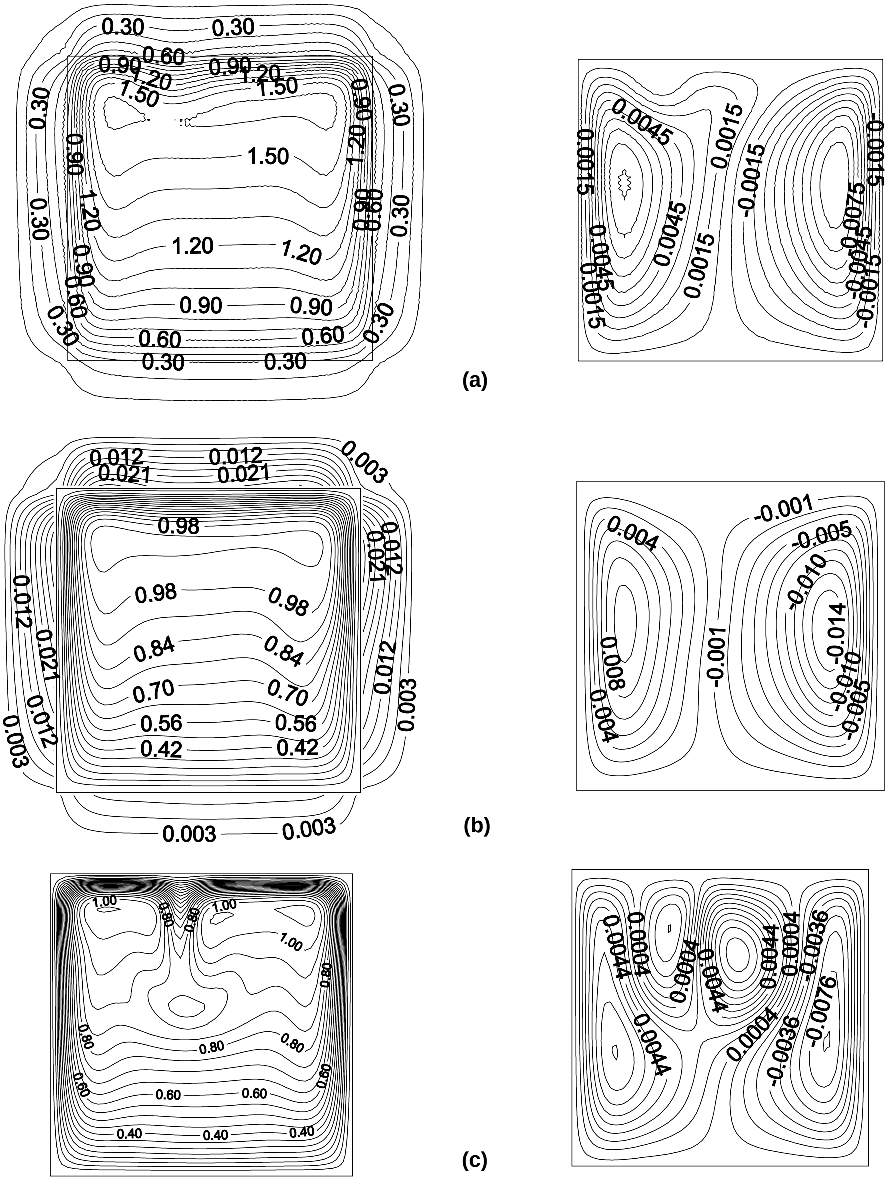

Fig. 3. Isotherms and streamlines for $Ra = 10^7$: (a) case 1; (b) case 2; (c) case 3.

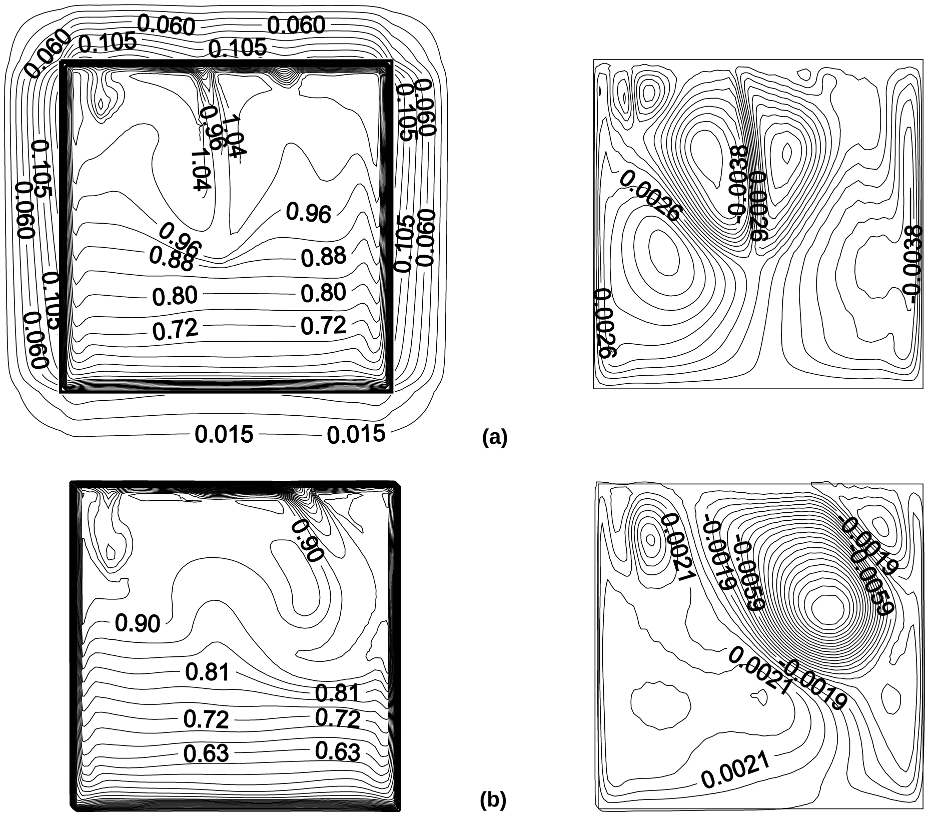

Fig. 4. Isotherms and streamlines for $Ra = 5.0 \times 10^{10}$: (a) case 2; (b) case 3.

Whereas the low value of θ_{max} is obtained for case 2 (Fig. 3(b)), indicating the efficient heat conduction from the solid walls. Streamlines in Fig. 3 also declare the same flow and heat transfer behaviour as discussed above.

Fig. 4 shows the isotherms and streamlines at $Ra = 5.0 \times 10^{10}$ for the cases 2 and 3. Temperatures in Figs. 4(a) and (b) are stratified in lower half of the enclosure. The flow is mainly located in the upper half of

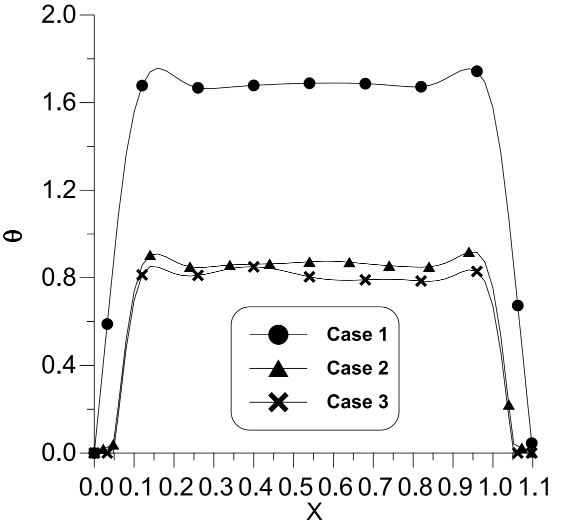

Fig. 5. Temperature distributions across the enclosure at $Y = 0.55$ for $Ra = 10^8$.

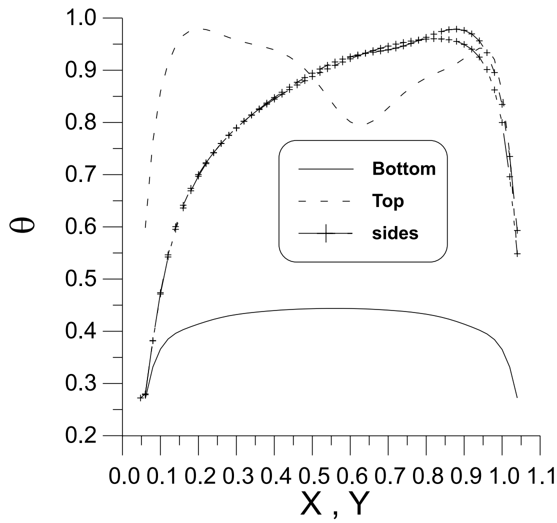

Fig. 6. Variation of interface temperature along the enclosure walls for $Ra = 10^8$, $A = 1.0$, $K = 1.0$.

the enclosure in Fig. 4(b). Thus maintaining the temperature stratification in the lower half of the Fig. 4(b).

In Fig. 5, temperature distribution across the enclosure at $Y = 0.55$ for Ra 10^8 has been illustrated. Much higher temperatures are obtained for case 1, while lowest temperatures are obtained for case 3. This indicates the difference of the heat transfer across the solid walls for the two cases. There is a large temperature difference across the wall for case 1, which reduces the heat flow through the wall. Temperature variation at interface is smooth for case 1 while it shows a significant change for cases 2 and 3. This is due to the difference of conductivity ratios for these cases.

For case 1, interface temperature distribution along the four walls for $Ra = 10^8$ have been shown in Fig. 6. Maximum temperature is obtained along the top wall while lowest temperature is obtained along the bottom wall. For side walls the temperature varies from that of bottom wall at lower end up to that of the top wall at the upper end. A dip in the top interface temperature indicates the position of the descending cold lobe of the fluid. Vertical velocity profiles at $Y = 0.55$ are shown in Fig. 7 for all three cases, at $Ra = 10^8$. Velocity distributions clearly show the descending boundary layers along the side walls. Maximum descending velocities along the side walls are obtained for case 2. Thus

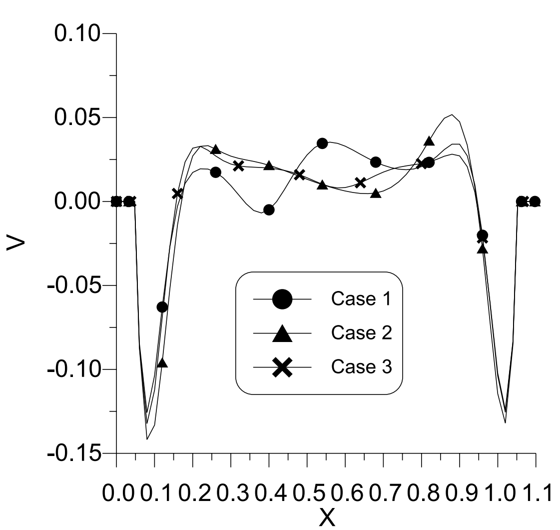

Fig. 7. Variation of V with X co-ordinate at $Y = 0.55$ for $Ra = 10^8$, for three cases.

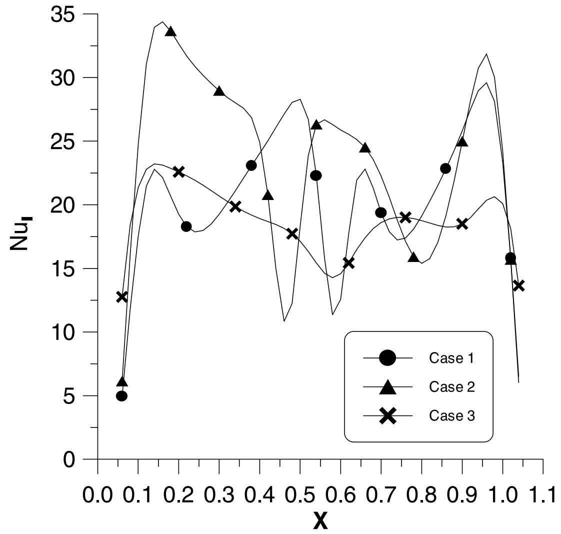

Fig. 8. Distribution of Nu_l at the top wall for the three cases for $Ra = 10^8$.

Table 4
Summary of final results for present analysis

Ra	K	Nu_a		
		Top	Sides	Bottom
1.0×10^7	1.0	12.37	10.43	5.67
	21.0	12.53	10.70	4.87
	∞	13.53	10.29	4.80
1.0×10^8	1.0	21.08	18.47	9.28
	21.0	22.31	18.06	6.02
	∞	23.14	17.56	5.87
1.0×10^9	1.0	35.92	35.72	23.89
	21.0	42.57	33.05	7.43
	∞	33.61	40.30	7.47
1.0×10^{10}	21.0	76.61	61.84	12.43
	∞	76.73	63.08	12.49
5.0×10^{10}	21.0	103.42	95.03	30.32
	∞	108.76	97.12	33.68
1.0×10^{11}	21.0	123.99	108.55	46.06
	∞	123.82	113.93	54.66
1.0×10^{12}	∞	187.48	183.80	146.62

indicating the efficiency of the heat extracted by the solid walls from the descending fluid.

4.2. Nusselt number

Local top wall nusselt numbers at $Ra = 10^8$ for the 3 cases considered are shown in Fig. 8. Maximum Nu_l is obtained for case 2, indicating sharp wall temperature gradient for this case. Nu_a values for the three cases and the simulations performed during present analysis are summarised in Table 4. As expected, Nu_a increases as Ra number is increased for all cases.

5. Conclusions

Transient conjugate free convection analysis for a square enclosure having thick walls has been performed. Results indicate a strong effect of the wall conduction for thick walled enclosure. It has been shown that a higher value of diffusivity ratio plays a significant role in cooling the fluid contained in the enclosure along with the conductivity ratio. Realistic values of conductivity ratio and thermal diffusivity ratio resulted in much lower fluid temperatures even when compared with very high conductivity ratio (∞) (cases 2 and 3, respectively). Flow patterns and isotherms for conjugate analysis show a great difference from that of conventional non-conjugate solutions reported in the open literature.

The main conclusion reached in the present study is about the importance of the conjugate analysis of the thick walled problems as it may give qualitatively different results from non-conjugate analysis.

Acknowledgements

This paper has been supported as a Ph.D. study by the Istanbul Technical University Research Fund, through grant 1190.

References

[1] U. Reineke, H.H. Steinberner, Turbulent buoyancy convection heat transfer with internal heat sources, in: Proceedings of the Sixth International Heat Transfer Conference, vol. 2, Toronto, 1978, pp. 305–310.

[2] A. Liaqat, A.C. Baytas, Heat transfer characteristics of internally heated liquid Pools at high Rayleigh numbers, Heat and Mass Transfer (in press).

[3] F.A. Kulacki, M.E. Nagle, Natural convection in a horizontal fluid layer with volumetric energy sources, Trans. ASME (1975) 98–103.

[4] A.A. Emara, F.A. Kulacki, A numerical investigation of thermal convection in a heat-generating fluid layer, J. Heat Transfer 102 (1980) 531–537.

[5] C.P. Tzanos, H.C. Dae, Numerical predictions of natural convection in a uniformly heated pool, Trans. Amer. Nucl. Soc. A 68 (1993) 496–498.

[6] R.F. Bergholz, Natural convection of a heat generating fluid in a closed cavity, Trans. ASME 102 (1980) 242–247.

[7] H.O. May, A numerical study of natural convection in an inclined square enclosure containing internal sources, Int. J. Heat Mass Transfer 34 (8) (1991) 919–928.

[8] A. Liaqat, A.C. Baytas, Heat transfer characteristics of internally heated pools at high Rayleigh numbers, Heat and Mass Transfer 36 (2000) 401–405.

[9] J.H. Lee, R.H. Goldstein, An experimental study on natural convection heat transfer in an inclined square enclosure containing internal energy sources, J. Heat Transfer 110 (1988) 345–349.

[10] R.R. Nourgaliev, T.N. Dinh, B.R. Sehgal, Effect of fluid Prandtl number on heat transfer characteristics in internally heated liquid pools with Rayleigh number up to 10^{12}, Nucl. Eng. Design 169 (1997) 165–184.

[11] L. WanLai, K.D. Carlson, C. Cing-Jen, Pressure boundary conditions of incompressible flows with conjugate heat transfer on nonstaggered grids part 1: methods, Numer. Heat Transfer A 32 (1997) 459–479.

[12] D.A. Kaminski, C. Prakash, Conjugate natural convection in a square enclosure effect of conduction in one of the vertical walls, Int. J. Heat Mass Transfer 29 (1986) 1979–1988.

[13] S.V. Patankar, in: Numerical Heat Transfer and Fluid Flow, McGraw-Hill, New York, 1980.

[14] H.K. Versteeg, W. Malalsekera, in: An Introduction to Computational Fluid Dynamics, The Finite Volume Method, Longman, New York, 1996.

[15] G.D. Vahl Davis, Natural convection of air in a square cavity: a bench mark numerical solution, Int. J. Num. Meth. Fluids 3 (1983) 249–264.

[16] J.L. Lage, A. Bejan, The *Ra–Pr* domain of laminar natural convection in an enclosure heated from the side, Numer. Heat Transfer A 19 (1991) 21–41.